

ELUCIDATING THE ROLE OF THE THERMAL BUDGET ON THE BULK DEGRADATION OF N-TYPE CZOCHRALSKI-GROWN UPGRADED METALLURGICAL-GRADE SILICON WAFERS DURING THE PROCESSING OF PHOSPHORUS-DOPED POLYSILICON CELLS

Rabin Basnet¹, Sieu Pheng Phang¹, Christian Samundsett¹, Di Yan¹, Chang Sun¹, Hieu T. Nguyen¹, Fiacre Emile Rougieux², and Daniel Macdonald¹

¹Research School of Electrical, Energy and Material Engineering, The Australian National University, Canberra, ACT 2601, Australia

²School of Photovoltaic and Renewable Energy Engineering, The University of New South Wales, Sydney, New South Wales, Australia

ABSTRACT: Upgraded Metallurgical-Grade (UMG) silicon is a promising low-cost feedstock material for silicon solar cells. However, UMG wafers are susceptible to high-temperature degradation due to the presence of a relatively high concentration of metallic (e.g., Fe, Cu, and Cr) and non-metallic impurities such as oxygen and carbon. In this case, high-temperature process steps such as boron diffusion and oxidation result in significant bulk degradation due to the formation of ring defects. This work aims to investigate the influence of high-temperature thermal processes on the formation of defects in n-type UMG-Cz wafers. Here, we focus on the thermal processes involved in the fabrication of single-boron diffusion and double-boron diffusion solar cells with phosphorus-doped polysilicon contacts on n-type UMG wafers. Using a combination of quasi-steady-state photoconductance lifetime testing, Fourier transform infrared spectroscopy for interstitial oxygen concentration measurement, and photoluminescence imaging, it is shown that the performance of the UMG-Cz solar cells was affected by the thermal budget used during the fabrication. With the *tabula rasa* step, the $i-V_{oc}$ of the UMG-Cz cells fabricated with single-boron diffusion increased from 650 mV to 690 mV. Further, the $i-V_{oc}$ of the *tabula rasa* treated UMG-Cz cells decreased to 630 mV after using double-boron diffusion process.

Keywords: *tabula rasa*, ring defects, upgraded metallurgical-grade silicon

1 INTRODUCTION

Upgraded Metallurgical-Grade (UMG) silicon is a promising low-cost feedstock material for silicon solar cells [1]. However, UMG-Cz wafers potentially have a relatively high concentration of metallic (e.g., Fe, Cu, and Cr) and non-metallic impurities (e.g., O and C) compare to electronic grade (EG) wafers purified via the Siemens process. Hence, UMG wafers are susceptible to high-temperature degradation, usually during oxidation or boron diffusion because of the activation of defects related to the oxygen precipitates and metallic impurities, which usually appear as ring defects. Thus it is crucial to avoid the formation of ring defects in the solar cell precursors. Several works have shown that the degradation due to oxygen precipitates can be mitigated by dissolving the grown-in OPN utilizing a pre-fabrication anneal, known as a *tabula rasa* (TR) step [2]–[5].

In this work, we have demonstrated the benefit of a TR step on the mitigation of bulk-degradation on the UMG-Cz wafers during the fabrication of solar cells with phosphorus-doped polysilicon as an electron selective contact. Further, we have investigated the impact of the increased thermal budget on the benefit of TR treatment.

2 EXPERIMENTAL DETAILS

The n-type UMG-Cz wafers were supplied by Apollon Solar in the framework of the PHOTOSIL project [6]. The UMG wafers contain a boron concentration $[B] = 1.3 \times 10^{16} \text{ cm}^{-3}$ and a phosphorus concentration $[P] = 1.7 \times 10^{16} \text{ cm}^{-3}$, and a carbon concentration $[C] = 1.0 \times 10^{16} \text{ cm}^{-3}$, as calculated from the secondary-ion mass spectrometry (SIMS). The interstitial oxygen concentrations $[O_i] = 6.3 \times 10^{17} \text{ cm}^{-3}$

were measured by Fourier transform infrared spectroscopy (FTIR) and were calibrated using SEMI MF standard 1188-1107. The commercially available float-zone (FZ) wafers had a doping concentration, $n_0 = [P] = 2.3 \times 10^{15} \text{ cm}^{-3}$, as determined by dark conductance measurements.

For cell fabrication convenience, 4-inch round UMG wafers were laser cut from the 6-inch pseudo-square wafers. Lifetime samples were prepared by dicing 6-inch wafers into four quarters. All samples were saw-damage-etched in Tetramethylammonium hydroxide (TMAH) solution to remove 10-12 μm from each side, with final thicknesses of 150 μm and 280 μm for the UMG and FZ wafers, respectively. Samples were cleaned using standard RCA cleaning steps prior to each high-temperature step. The TR step in this work was performed in an oxygen ambient at 1000 °C for 30 min with loading and unloading at 700 °C and ramp up and down rates of 15 °C/min. To assess the benefit of the TR step, samples were divided into two groups; as-grown (no pre-fabrication treatment) and TR. These two groups of samples were then subjected to the solar cell fabrication process involving the single-boron diffusion (SBD), as shown in Fig. 1.

Further, to assess the impact of the thermal budget, some of the TR-treated UMG-Cz and FZ wafers were used to fabricate selective-emitter solar cells with the double-boron diffusion (DBD) steps, as shown in Fig. 1. To understand the evolution of bulk degradation, the solar cell fabrication processes were divided into three stages, as shown in Fig. 1. The lifetime samples were used to calculate the 1-sun implied open-circuit voltage ($i-V_{oc}$) measured from injection-dependent lifetimes at each stage. Stage 1 was the starting step of cell fabrication where the wafers were grouped as the as-grown and TR-treated wafers. In stage 2, the diffusion

masks (DM) were deposited, and boron diffusions were performed. The SBD process had only one DM and boron diffusion, whereas the DBD process had two DM and boron diffusion steps, as shown in Fig. 1. For the detail description of the DM deposition and boron diffusions, please refer to [7]. In stage 3, the full-area rear phosphorus-doped polysilicon layers were formed with further details in Ref [7]. Then the front AlO_x/SiN_x stacks were deposited by atomic layer deposition (Benq TFS200) and PECVD (Roth & Rau AK400) for front surface passivation and anti-reflection, respectively.

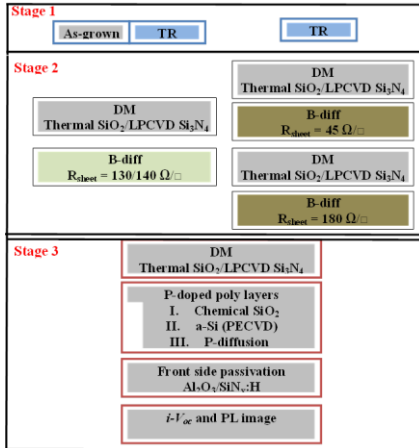


Fig. 1: Schematic of the solar cell fabrication processes used in this work.

All lifetime samples were etched back to remove diffusion masks and diffused layers using hydrofluoric acid (HF) dip and TMAH etch. For the lifetime measurements, the samples were passivated with SiN_x layers using PECVD. Carrier lifetimes were measured using the quasi-steady state photoconductance and transient photoconductance decay techniques with a WCT-120 tool from Sinton Instruments [8]. The carrier lifetimes of the UMG wafers were corrected using carrier mobility values for compensated silicon from Schindler's mobility model [9]. Photoluminescence (PL) images were captured using an LIS-R1 PL imaging tool from BT imaging [10].

3 RESULTS AND DISCUSSION

3.1 SBD (as-grown vs. TR-treated sample)

Fig. 2 (a) illustrates the thermal budget involved in the fabrication of solar cells with the SBD process. As expected, boron diffusion was the step with the highest thermal budget. Fig. 2 (b) and (c) show the 1-sun implied open-circuit voltage (*i*-V_{oc}) derived from the injection-dependent carrier lifetimes measurements for both the UMG and FZ wafers. The as-grown UMG-Cz wafers had the lowest average *i*-V_{oc} of 680 mV and increased to 727 mV after the TR step in stage 1, as shown in Fig. 2 (b). The significant improvement in *i*-V_{oc} highlights the importance of pre-fabrication treatments for low-quality materials such as UMG silicon. It shows that the UMG-Cz has the potential to achieve a similar *i*-V_{oc} to FZ wafers after appropriate pre-treatments. After depositing DM and boron diffusion step, in stage 2, we observed bulk degradation in both the as-grown and TR-treated UMG wafers. The degradation was severe in the as-grown wafers, as *i*-V_{oc} reduced to 630 mV. However, the

degradation was not severe in the TR-treated wafers with *i*-V_{oc} maintaining in the 680 mV range. The bulk degradation was mostly due to the growth/activation of the pre-existing OPN in the as-grown and formation of new OPN in the TR-treated wafers caused by the high-thermal budget during the boron diffusion process. This is supported by the further loss of [O_i] in stage 2, as shown in Fig. 3(c). Further, the degradation can be contributed by process contamination, as in-situ oxidation during boron diffusion does not provide any impurity gettering [11]. Fortunately, the phosphorus-doped polycrystalline silicon contacts formed on the rear side is known to provide strong gettering effects without any additional thermal budget [12], [13]. As a result, average *i*-V_{oc} improved to 650 mV and 690 mV for the as-grown and TR-treated UMG wafers at stage 3, as shown in Fig. 2 (b). The low *i*-V_{oc} of the as-grown UMG-Cz wafers was due to ring defects, as shown in the PL image in Fig. 3. Hence the as-grown UMG-Cz could not sustain the thermal budget involved in the SBD process, but the TR-treated wafers survived. However, the impact of the SBD process's thermal budget on the FZ was minimal. The benefit of the TR step was also negligible as the average *i*-V_{oc} for the as-grown, and TR-treated FZ wafers were 707 and 709 mV, respectively, as shown in Fig. 2 (c).

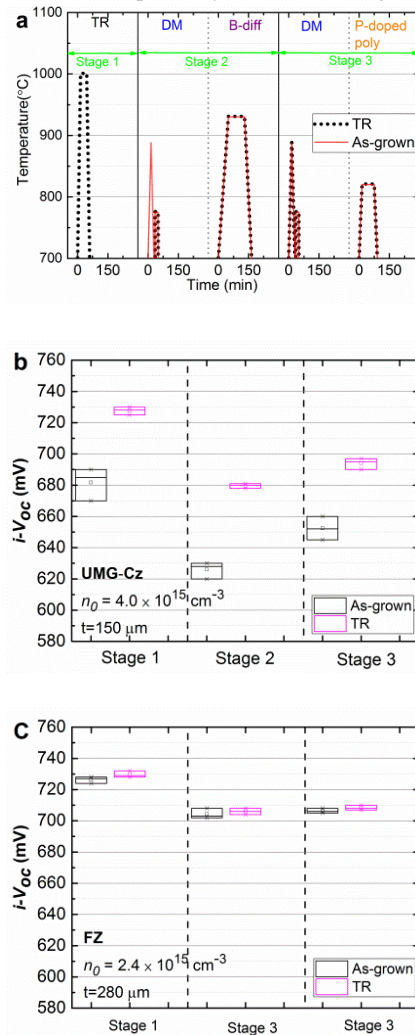


Fig. 2: (a) Thermal budget associated with the three stages of solar cell fabrication involving SBD process. The duration indicates the total time that samples

subjected to the given temperature. The 1-sun $i-V_{oc}$ extracted from the effective minority-carrier lifetime measurements, illustrating the evolution of bulk quality at three different stages on n-type (b) UMG-Cz and (c) FZ wafers.

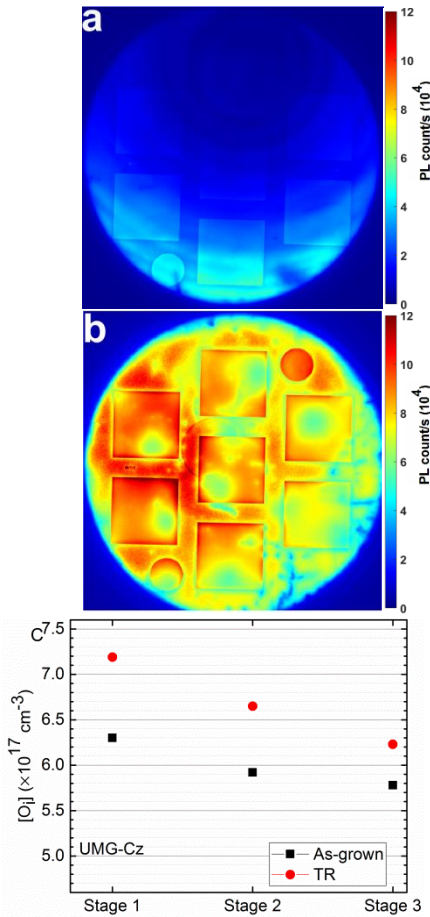


Fig. 3: PL images of the 4-inch UMG-Cz wafers at stage 3 of SBD process (a) as-grown and (b) TR-treated wafers. PL images were captured at an illumination intensity of 0.5 suns. (c) Average interstitial oxygen concentration measured by FTIR present in the UMG wafers after each stage, as shown in Fig. 1.

3.2 DBD vs. SBD (TR-treated sample)

The thermal budget involved in the DBD solar cell process is shown in Fig. 4 (a). The high thermal budget due to extra boron diffusion and DM steps in the DBD process caused the formation of ring defects even in the TR treated UMG-Cz wafers, as shown in the PL image in Fig.4(b). As a result, the average $i-V_{oc}$ of only 630 mV was achieved for the UMG-Cz wafers. This is significantly smaller than the $i-V_{oc}$ of 690 mV achieved with the SBD process in the TR-treated UMG-Cz wafer. However, the FZ wafer achieved the average $i-V_{oc}$ of 715 mV, which is higher than the SBD process. In general, higher $i-V_{oc}$ is expected from the selective emitter cell structure due to less contact recombination and lower contact resistivity [14]. As expected, the FZ wafer achieved the average $i-V_{oc}$ of 715 mV with the DBD process, which is higher than the SBD process.

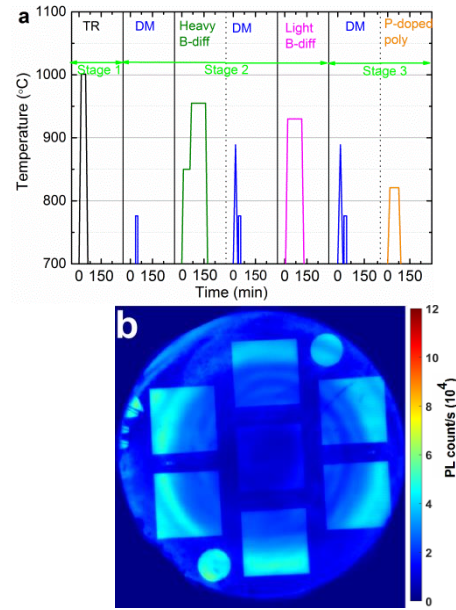


Fig. 4. (a) Thermal budget associated with the solar cell fabrication involving double-boron diffusion process. The duration indicates the total time that samples subjected to the given temperature. (b) PL images of the 4-inch TR-treated UMG-Cz wafers at stage 3 of DBD process. PL images were captured at an illumination intensity of 0.5 suns.

The results from the above two sections showed that the TR step was not a permanent solution for the prevention of ring defects in these UMG-Cz wafers. The TR steps provide only a specific window of safe duration for a given thermal budget, known as the incubation time. The incubation time provided by the TR step in this work was enough to withstand the thermal budget of the SBD process on the UMG-Cz wafers. However, the addition of extra boron diffusion and diffusion mask steps in the DBD process caused the formation of the ring defects making the TR step ineffective. The incubation time depends on the several factors such as thermal budget, initial $[O_i]$ and $[C]$, and intrinsic point defects concentrations, all of which affect the reformation of oxygen precipitates in silicon wafers [15]–[17]. These UMG-Cz wafers have a relatively high concentration of $[C]$ and vacancy, which enhanced the oxygen precipitation; as a result, reducing the incubation time.

4 CONCLUSION

In this work, we observed that the pre-fabrication treatment like *tabula rasa* helps to improve the bulk lifetimes and mitigates the subsequent thermal degradation on the UMG-Cz wafers. This resulted in a gain of 50 mV of $i-V_{oc}$ in the SBD process of solar cells. However, we also discovered that ring defects formed even on the TR-treated UMG-Cz wafers after increasing the thermal budget using the DBD process. This caused the reduction of $i-V_{oc}$ by 60 mV in the DBD process in comparison to the SBD process of phosphorus-doped polysilicon solar cells. As expected, we did not observe any significant degradation on the FZ solar cells. With the selective emitter structure (DBD process), the FZ solar cells achieved higher $i-V_{oc}$ in comparison to the homogenous emitter (SBD process). Hence the selection

of the thermal budget significantly impacts the performance of the solar cells based on the low-quality materials like the UMG-Cz wafers. This work also opens up several avenues to reduce bulk degradation of the low-quality material.

4 ACKNOWLEDGEMENT

This work has been supported by the Australian Renewable Energy Agency (ARENA) through the Australian Centre for Advanced Photovoltaics (ACAP), and projects RND009 and RND017. Apollon solar are acknowledged for providing the UMG wafers.

5 REFERENCES

- [1] P. Zheng, F.E. Rougieux, X. Zhang, et al., *IEEE J. Photovoltaics*, 7 (2017), pp. 58–61.
- [2] B. Sopori, P. Basnyat, S. Devayajanam, et al., *IEEE J. Photovoltaics*, 7 (2016).
- [3] R. Basnet, F.E. Rougieux, C. Sun, et al., *IEEE J. Photovoltaics*, 8 (2018), pp. 990–996.
- [4] D. Walter, B. Lim, R. Falster, J. Binns, and J. Schmidt, *Processing of the 28th European Photovoltaic Solar Energy Conference and Exhibition*, (2013), pp. 699–702.
- [5] V. LaSalvia, A. Youssef, M.A. Jensen, et al., *Prog. Photovoltaics Res. Appl.*, 27 (2019), pp. 136–143.
- [6] R. Einhaus, J. Kraiem, S. Martinuzzi, and M. C. Record, *Proceedings of the 21st European Photovoltaic Solar Energy Conference (PVSEC '06)*, (2006), pp. 580–584.
- [7] R. Basnet, S.P. Phang, C. Samundsett, et al., *Sol. RRL*, 0 (2019).
- [8] R. A. Sinton and A. Cuevas, *Appl. Phys. Lett.*, 69 (1996), pp. 2510–2512.
- [9] F. Schindler et al., in *Solar Energy Materials and Solar Cells*, 106 (2012), pp. 31–36.
- [10] T. Trupke, R. Bardos, M. Schubert, and W. Warta, *Appl. Phys. Lett.*, 89 (2006), pp. 044107–044107.
- [11] S. P. Phang, W. Liang, B. Wolpensinger, M. A. Kessler, and D. MacDonald, *IEEE J. Photovoltaics*, 3 (2013), pp. 261–266.
- [12] A. Y. Liu, D. Yan, S. P. Phang, A. Cuevas, and D. Macdonald, *Sol. Energy Mater. Sol. Cells*, 179, (2018), pp. 136–141.
- [13] A. Liu, D. Yan, J. Wong-Leung et al., *ACS Appl. Energy Mater.*, 1 (2018), pp. 2275–2282.
- [14] U. Jäger, S. MacK, C. Wufka, A. Wolf, D. Biro, and R. Preu, *IEEE J. Photovoltaics*, 3 (2013), pp. 621–627.
- [15] R. Falster and V. V. Voronkov, *Mater. Sci. Eng. B Solid-State Mater. Adv. Technol.*, 73 (2000), pp. 87–94.
- [16] S. Zhang, M. Juel, E. J. Vreliid, and G. Tranell, *J. Cryst. Growth*, 411 (2015), pp. 63–70.
- [17] F. Shimura, *J. Appl. Phys.*, 59 (1986), pp. 3251–3254.